

Nd:YAG 레이저의 근적외선과 자외선 펄스를 이용한 NiP 하드디스크 기층의 세척

Cleaning of Nip Hard Disk Substrate Using Near-Infrared and Ultraviolet Irradiation of Nd:Yag Laser Pulses

포항공과대학교 기계공학과 김동식

Abstract: This paper introduces a cleaning process for removing submicron-sized particles from NiP hard disk substrates by the liquid-assisted laser cleaning technique. Measurements of cleaning performance and time-resolved optical diagnostics are performed to analyze the physical mechanism of contaminant removal. The results reveal that nanosecond laser pulses are effective for removing the contaminants regardless of the wavelength and that a thermal mechanism involving explosive vaporization of liquid dominates the cleaning process.

I. INTRODUCTION

Effective contamination control and development of an efficient cleaning tool are important in microelectronics industry (Mittal, 1988). Especially, contamination by submicron-sized particles has become a critical issue in semiconductor-device and data-storage industry. As the cleaning efficiency of a common cleaning tool is proportional to the surface area or volume of the contaminants, removal of a submicron particle requires advanced technology to overcome the strong adhesion force. For example, Fig. 1 demonstrates the adhesion forces acting on an alumina (Al_2O_3) particle on pure Ni surfaces. In the calculation it has been assumed that the particle-surface spacing is 4 Å on the basis that the value is comparable to a typical value of molecular spacing. In the figure, the adhesion forces have been normalized by gravitational force, i.e., weight of an alumina particle. It is noted that application of a liquid film on the contaminated solid surface weakens the bond between contaminants and solid surfaces. If a particle is immersed in liquid, van der Waals force is in general reduced by the electromagnetic shielding effect. Furthermore, the capillary adhesion force is entirely eliminated in the wet process. Therefore, the liquid-assisted laser cleaning process has inherent advantage over dry processes.

In the present work, laser cleaning of submicron alumina particles on NiP hard disk substrates are performed by Q-switched Nd:YAG laser pulses ($\lambda=1064$ and 355 nm, FWHM=6 ns). Previous studies employing an excimer laser have shown that nanosecond laser pulse is effective for submicron particles and that the cleaning efficiency depends on a number of parameters, such as laser fluence, pulse width, wavelength, angle of incidence, thickness of the deposited liquid film, and properties of puffing liquid (Tam, 1992; Park, 1994). The present study utilizes a Nd:YAG laser for cleaning NiP hard disk surfaces. It is obvious that laser cleaning using a solid-state laser is more attractive than excimer laser cleaning since it requires relatively low implementation cost and easy maintenance. In addition to the practical aspects, this work can enlighten the role of laser wavelength by performing the laser cleaning test at near-IR (infrared) and UV (ultraviolet) wavelengths ($\lambda=1064$ nm and 355 nm). Based on the obtained experimental results, discussions are made on the physical mechanisms of liquid-assisted laser cleaning.

II. EXPERIMENTS

The schematic diagram of the experiment setup is shown in Figure 2. A Q-switched Nd:YAG laser beam irradiates the substrate and vaporize the thin liquid film. This rapid phase-change process depends on several parameters such as laser fluence, pulse duration, substrate absorption coefficient, and laser incidence angle. In this experiment, the laser beam is directed onto the sample at an incidence angle of 40°. The thin liquid film is deposited by a process employing puffing and condensation of the saturated vapor. A heater is used to maintain the liquid inside the source container at a temperature slightly below the saturation point. The liquid-film deposition lasts for about 200 ms (determined from the process optimization results). After an additional elapsed time of 200 ms, the Nd:YAG laser is fired onto the target substrate. In addition to the cleaning test, *in-situ* measurements of optical reflectance are carried out to characterize the physical mechanisms of laser cleaning, as depicted in Fig. 2. Reflectance of a HeNe probe beam ($\lambda=633$ nm) is measured at an incidence angle of 10°. It is noted that the reflectance measurements have been conducted without depositing the contaminant particles to probe the vaporization kinetics only.

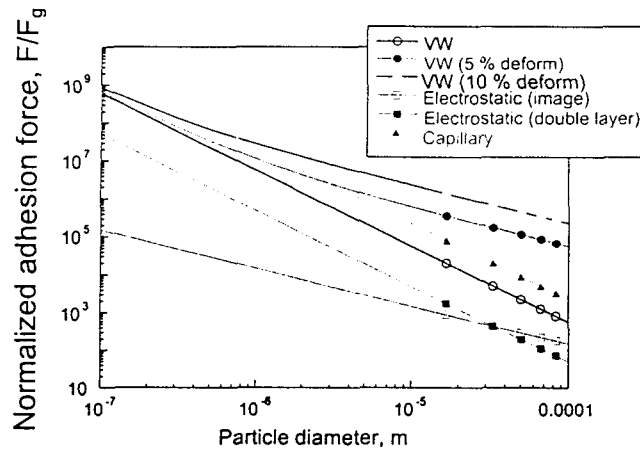


Fig. 1 Adhesion forces between a spherical alumina (Al_2O_3) particle and a Ni surface are normalized by the gravitational force (particle weight). Van der Waals force has been estimated for three different cases, assuming that the particle experiences 0, 5, or 10 % of volume deformation in the contact region.

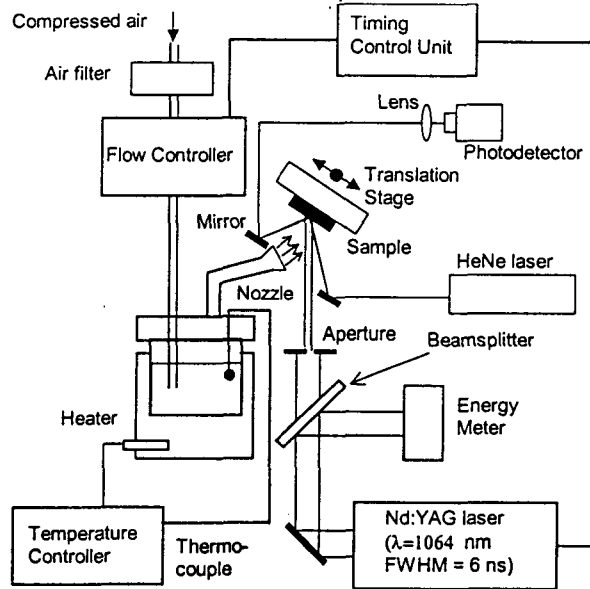


Fig. 2 Schematic diagram of the Nd:YAG laser (variable wavelength, FWHM=6 ns) cleaning systems.

III. RESULTS AND DISCUSSION

The threshold laser fluences for removing submicron alumina (Al_2O_3) particles have been obtained by analyzing the microscope images before and after the laser pulse irradiation. Since the size of the contaminant particles (Al_2O_3) is not uniform (mean diameter $0.3 \mu\text{m}$), the particle removal threshold is not uniquely determined. Large particles or aggregates are easily fragmented and detached at a relatively low laser fluence. Experimental results confirm this trend, showing that large particles or aggregates are removed at much lower laser fluences than those required for complete removal of small particles. The minimum laser fluence for removal of micron-sized or larger contaminants was lower by a factor of about two than the fluence necessary for complete removal of $0.3 \mu\text{m}$ particles. Accordingly, the laser cleaning threshold in the present paper is defined as the laser fluence required for complete removal of the contaminants. Figures 3 exhibits a typical laser cleaning result. The measured cleaning threshold is 86 and 63 mJ/cm^2 for $\lambda=1064$ and 355 nm , respectively.

The fact that both the near-IR and the UV wavelengths are effective for particle removal suggests that

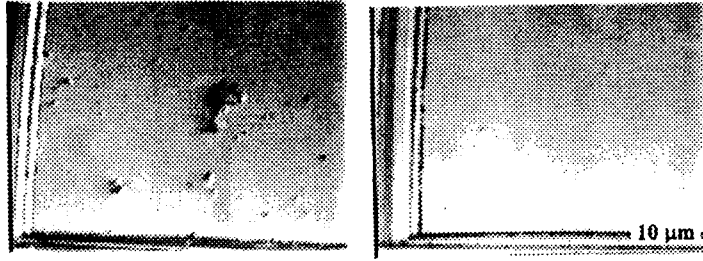


Fig. 3 Optical microscope photographs of a NiP hard disk surface contaminated with $0.3 \mu\text{m}$ -sized (average) alumina particles and the same spots after 10 steam Nd:YAG laser pulses ($\lambda=1064 \text{ nm}$, 86 mJ/cm^2).

photochemical mechanism plays a rather minor role in the cleaning process. It is noted that the photon energy at $\lambda=1064 \text{ nm}$ is only 1.2 eV (3.5 eV at $\lambda=355 \text{ nm}$). The difference in the cleaning thresholds for the two wavelengths can be explained by considering the spectral dependence of optical properties of NiP surface, which were determined by spectroscopic ellipsometry over the range from 300 to 1200 nm . The surface reflectivity $R=0.64$ at $\lambda=1064$ and is only 0.39 at $\lambda=355 \text{ nm}$. In both cases, the optical penetration depths ($1/\alpha = \lambda/4\pi k = 20 \text{ nm}$ at $\lambda=1064 \text{ nm}$ and 18 nm at 355 nm , α : absorption coefficient, k : extinction coefficient) are much smaller than the thermal penetration depth $\sim \sqrt{4\kappa\tau} = 300 \text{ nm}$ (κ : thermal diffusivity, τ : laser pulse width). Therefore, the temperature increase in the heat-affected zone is proportional to the absorptivity $A=1-R$ to a first order approximation. Assuming that the cleaning threshold depends only on the maximum surface temperature obtained during the cleaning process, the ratio of laser cleaning threshold at the IR wavelength to that at the UV wavelength can be estimated by the absorptivity ratio. The ratio $F_{th}(\lambda=355 \text{ nm})/F_{th}(\lambda=1064 \text{ nm})$ obtained in the present work is 0.73 while the ratio $A(\lambda=355 \text{ nm})/A(\lambda=1064 \text{ nm})$ is 0.59 . The uncertainty associated with the laser fluence could be one of the sources of this discrepancy. The threshold laser fluences are in fact average values over ten pulses. The maximum fluctuation of the laser pulse energy is $\pm 7\%$ of the mean value for the frequency-tripled harmonic compared to $\pm 2\%$ for the fundamental. The maximum surface temperature induced by the threshold energy is much lower than the melting temperature of NiP ($\approx 1200 \text{ K}$). This eliminates the possibility of laser-induced damage during the cleaning process. The damage threshold for a surface coated with a liquid film is about 115 mJ/cm^2 and for a dry surface it drops to about 100 mJ/cm^2 . The laser beam has a fit-to-Gaussian spatial profile within 95% .

Among the many parameters affecting the laser-cleaning performance, the laser beam incident angle plays a critical role. Experiments conducted using the near-IR beam at a normal incidence angle for 1064 nm reveal that complete removal of $0.3 \mu\text{m}$ -sized alumina particles is not possible and only large (micron-sized) particles begin to detach from the surface at 53 mJ/cm^2 .

The kinetics of explosive vaporization processes has been studied by detecting optical reflectance signals. The signal characterizes the effect of light scattering and interference in the liquid condensation/vaporization process. Figure 4 (a) displays a typical reflectance signal obtained during the liquid film deposition/vaporization process without laser-pulse irradiation. In the figure, the interference pattern corresponds to the variation of liquid film thickness. Accordingly, the liquid-film thickness is of the order of the wavelength of the probe beam. The thickness can also be estimated from the overall recovery time of the reflectance signal τ , i.e., $\sim 1 \text{ s}$ in Fig. 4 (a). By assuming that the process is governed by mass diffusion at a constant (room) temperature, the mass flux j_l can be expressed as $j_l = -\rho D_{l-air} \partial m_l / \partial x|_{x=0} = \rho m_l \sqrt{D_{l-air} / t\pi}$ (ρ , density; D_{l-air} , binary diffusion coefficient between the liquid and air; m_l , liquid concentration). Therefore, the total mass flux over a period of τ becomes $2\rho m_{ls} \sqrt{D_{l-air} \tau / \pi}$, where the mass concentration m_{ls} at the liquid-air interface is expressed as $m_{ls} = P_{sat}(T_\infty) / P_\infty$ (P_{sat} , saturation pressure; T_∞ ambient temperature; P_∞ ambient pressure). Assuming that the liquid film is composed of pure water ($D_{l-air} = 2.6 \times 10^{-5}$), an estimated thickness of $0.36 \mu\text{m}$ is obtained. It is noted that the above analysis assumes a pure diffusion process under isothermal condition. In addition, the analysis neglects the effect of external flow unavoidably induced by the puffing (spraying) action. Consequently, it is reasonable to regard the estimated value as a lower bound of the liquid film thickness.

Similar reflectance signals are obtained over the period of $\sim 1 \text{ s}$ in the presence of a laser pulse as well, indicating that the liquid film removal is driven mainly by natural evaporation (mass diffusion) of the liquid,

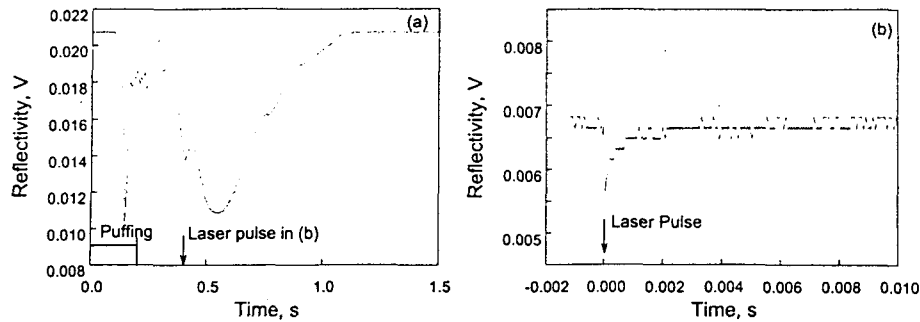


Fig. 4 The HeNe laser ($\lambda=633$ nm) reflectance signal (a) during the puffing process without laser-pulse irradiation (puffing duration = 200 ms) and (b) after a Nd:YAG laser pulse ($F=79$ mJ/cm², $\lambda=1064$ nm, FWHM=6 ns).

not by the laser pulse. However, there exists a short-term reflectance drop over ~ 1 ms right after the laser-pulse irradiation. Figure 4 (b) represents the short-term reflectance transient at a laser fluence above the liquid-vaporization threshold. These short-term reflectance signals have been measured for several laser fluences. At low laser fluences below the liquid vaporization threshold, no rapid transient of reflectance signal is observed. Once the laser fluence reaches the threshold value, a sharp drop of the signal appears due to vaporization. By measuring the short-term reflectance signal, the vaporization threshold has been determined to be 27 and 52 mJ/cm² for $\lambda=355$ and 1064 nm, respectively. Strong absorption of laser energy at $\lambda=355$ nm explains the low vaporization threshold. In Fig. 4 (b), the localized reflectance drop occurs over a period of about 1 ms. In contrast, the time scale of nanosecond laser induced vaporization in bulk liquid is typically on the order of one microsecond (Yavas *et al.*, 1993; Kim *et al.* 1996). It is thus clear that the reflectance drop in Fig. 4 (b) corresponds to the ablation plume ejection after the laser pulse. The contaminant particles detached from the surface during the process of explosive bubble nucleation are permanently removed by the subsequent vapor-plume ejection over a time scale of ~ 1 ms. It is interesting to compare the vaporization phenomena with cleaning effect. The threshold laser fluence for large (micron-sized) particle removal was 53 mJ/cm² in the case of normal incidence of Nd:YAG laser beam. The fluence is close to the explosive-vaporization threshold under the same condition, which further corroborates the hypothesis that thermophysical mechanism (explosive vaporization due to temperature increase) largely dominates the cleaning process of submicron particle removal.

IV. CONCLUSION

This work demonstrates that effective removal of submicron-sized contaminants from NiP hard disk substrates can be achieved at moderate laser fluences by the liquid-assisted laser cleaning technique. Both near-IR and UV laser pulses removed 0.3 μm alumina particles from the surface without causing a damage. *In-situ* detection of optical reflectance in the process of liquid-assisted laser cleaning confirms that there is a strong correlation between the particle-removal threshold and the onset of vaporization (bubble-nucleation). It is concluded that the cleaning process is largely driven by the thermal mechanism involving explosive vaporization of liquid.

V. REFERENCES

- Mittal, K. L. ed., *Particles on Surfaces 1: Detection, Adhesion, and Removal*, Plenum Press, New York, 1988.
- Kim, D., Park, H. K., and Grigoropoulos, C. P., 1996, "Interferometric Study on the Growth of Pulsed-Laser-Generated Submicron Bubble Layer on a Solid Surface," presented at the 1996 ASME National Heat Transfer Conference, Houston, HTD-Vol. 326, pp. 69-77.
- Park, H. K., Grigoropoulos, C. P., Leung, W. P., and Tam, A. C., 1994 a, "A Practical Excimer Laser-Based Cleaning Tool for Removal of Surface Contaminants," *IEEE Transactions of Components, Packaging, and Manufacturing Technology - Part A*, Vol. 17, pp. 631-643.
- Tam, A. C., Leung, W. P., Zapka, W., and Ziemlich, W., 1992, "Laser-Cleaning Techniques for Removal of Surface Particulates," *Journal of Applied Physics*, Vol. 71, pp. 3515-3523.
- Yavas, O., Leiderer, P., Park, H. K., Grigoropoulos, C. P., Poon C. C., Leung, W. P., Do, N., and Tam, A. C., 1993, "Optical Reflectance and Scattering Studies of Nucleation and Growth of Bubbles at a Liquid-Solid Interface Induced by Pulsed Laser Heating," *Physical Review Letters*, Vol. 70, pp. 1830-1833.